ICE DEPTHS CALCULATIONS ON MARS AT THEMIS RESOLUTION. J. Buz[1], C. S. Edwards[1], S. Piqueux[2], [1]Northern Arizona University Department of Astronomy and Planetary Science, Flagstaff, AZ 86011, [2]Jet Propulsion Laboratory, California Institute of Technology. Contact: jennifer.buz@nau.edu

Introduction: Orbital and lander missions demonstrated that the high latitude regions of Mars have shallow subsurface ice [1–6]. Recent studies using thermophysical modeling have shown that shallow ice is widespread in both the mid and high latitudes [e.g., 7]. This ice is critical for both understanding the history of volatile transport and for future mission planning and in-situ resource utilization.

The thermal inertia of massive or pore-filling water ice is particularly high, significantly altering surface temperature patterns. Using repeat observations taken by the Thermal Emission Imaging System (THEMIS) and Mars Climate Sounder (MCS) at different seasons enables high resolution calculations of the thermophysical properties of the surface, in particular the thermal inertia, and the presence of subsurface ice [e.g., 8]. Furthermore, it is now possible to estimate the depth to any ice-rich layer found. Modification of previous ice depth calculation techniques [8–10] for use with THEMIS and MCS have enabled global mapping and mapping at high resolution [7].

Methods: We use the KRC numerical thermal model in conjunction with a DaVinci Interface (krc.mars.asu.edu) for thermophysical calculations [11]. A particular season, here called L_s*, exists where the surface temperature is primarily influenced by the top-layer thermal inertia (Figure 1). We use MCS and THEMIS observations during this season to calculate the thermal inertia of the surface (for details on this model see section S1 in Piqueux et al., 2019 [7]).

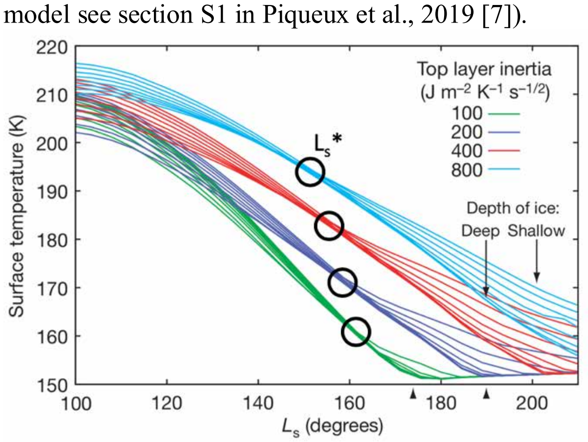

Figure 1
Modification of Figure 1 from Bandfield [8] indicating crossover point, L_s*, where surface temperature is primarily affected by top layer thermal inertia and only weakly by buried ice depth.

We assume a two-layered geometry of dry soil on top of a water rich layer [e.g., 7,9]. We then find regions where two overlapping THEMIS nighttime images exist, one which was acquired during L_s* and the other which was acquired at $\Delta L_s > 100°$. We use an ISIS mosaicking pipeline [12] to crop the images to the overlapping region and to create common image and pixel footprints.

We use the band 9 (12.57µm) brightness temperature of the THEMIS image acquired during L_s*, latitude, local time of observation, L_s, slope, albedo, dust opacity, elevation, and azimuth as inputs into the KRC thermal model to calculate the thermal inertia of the surface. We then generate a look-up table for surface temperatures at the second L_s using varying ice depths between 0.06 and 1.2 seasonal skin depths (Figure 2). A thermal inertia of 2261 is used for the second layer, following Bandfield [9]. We extrapolate using this table to estimate the ice depth.

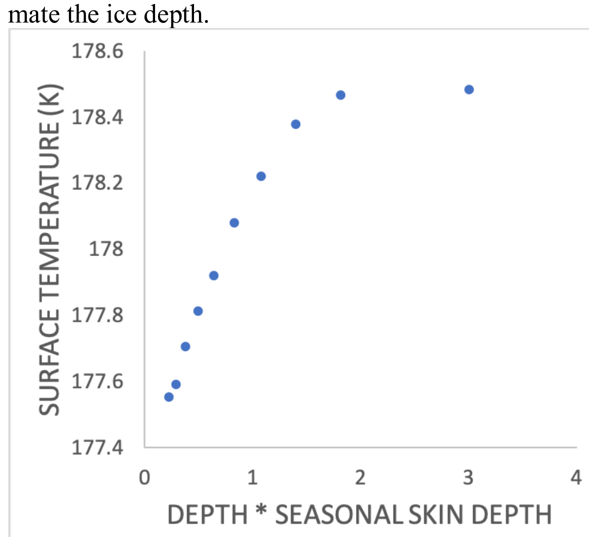

Figure 2
Effect of depth-to-ice rich layer on surface temperature.

Preliminary Results: We have focused our calculations on mid latitude regions previously found to variable subsurface ice depths [7]. Within these regions we have identified 550 overlapping THEMIS image pairs which meet our L_s requirements. We have computed the surface level thermal inertia and look-up tables for ~100 of these image pairs. For approximately 10% of these image pairs our methodology works without modification (Figure 3). For the other regions, however, our non-L_s* THEMIS image band 9 surface temperature has been up to 3 K above or below our look-up table values.

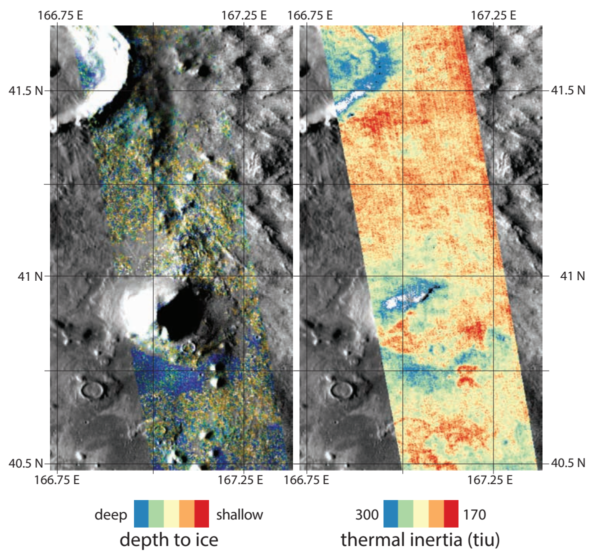

Figure 3: Figure from Piqueux et al. (2019). Ice depth varies with both albedo and thermal inertia of the surface.

Discussion: We find that thermal inertia and albedo are strong influences on ice depth and that ice depth varies significantly locally. These results will be necessary for future mission planning and in-situ resource utilization.

Future Work: MCS derived absolute surface temperatures are likely more accurate than the THEMIS band 9 surface temperatures due to differences in instrument calibration procedures and performances and instrument drift within THEMIS that have been well documented (~3K). Therefore, we will tie our calculations to MCS derived surface temperatures by modeling the thermal inertia using MCS, calculating the surface temperature using this thermal inertia at both Ls* and non-Ls*, and then subtracting the difference between this modeled surface temperature and the overlapping THEMIS derived surface temperature. Depth to ice will then be calculated at higher THEMIS resolutions with equivalent accuracy as the relative temperature uncertainties are much smaller (~<0.5K) Results will be presented.

Acknowledgements: Part of this work was performed at the Jet Propulsion Laboratory, California Institute of Technology, under a contract with NASA. NASA grants Solar System Workings 15-SSW15_2-0058 and Mars Data Analysis Program 14-MDAP14_2-0017 also provided support. Government support acknowledged.

References: [1] Feldman W. C. et al. (2004) *J. Geophys. Res. Planets* **109**, DOI 10.1029/2003JE002160.
[2] Boynton W. V et al. (2002) *Science (80-.).* **297**, 81 LP – 85.
[3] Mitrofanov I. G. et al. (2004) *Sol. Syst. Res.* **38**, 253–257.
[4] Mellon M. T. et al. (2009) *J. Geophys. Res. Planets* **114**, DOI 10.1029/2009JE003417.
[5] Smith P. H. et al. (2009) *Science (80-.).* **325**, 58 LP – 61.
[6] Arvidson R. E. et al. (2009) *J. Geophys. Res.* **114**, DOI Artn E00e02 10.1029/2009je003408.
[7] Piqueux S. et al. (2019) *Geophys. Res. Lett.* , DOI 10.1029/2019GL083947.
[8] Bandfield J. L. (2007) *Nature* **447**, 64.
[9] Bandfield J. L. and Feldman W. C. (2008) *J. Geophys. Res. Planets* **113**, DOI 10.1029/2007JE003007.
[10] Mellon M. T. et al. (2008) *J. Geophys. Res. Planets* **113**, DOI 10.1029/2007JE003067.
[11] Kieffer H. H. (2013) *J. Geophys. Res. Planets* **118**, 451–470.
[12] Edwards C. S. et al. (2011) *J. Geophys. Res. Planets* **116**, DOI 10.1029/2010JE003755.